Compressed supersymmetry after 1 fb^{-1} at the Large Hadron Collider

Thomas J. LeCompte and Stephen P. Martin

Compressed supersymmetry after 1 fb^{-1} at the Large Hadron Collider

Thomas J. LeCompte[1] and Stephen P. Martin[2,3,4]

1) Argonne National Laboratory, Argonne IL 60439, USA

2) Department of Physics, Northern Illinois University, DeKalb IL 60115, USA

3) Fermi National Accelerator Laboratory, P.O. Box 500, Batavia IL 60510, USA

4) Kavli Institute for Theoretical Physics, University of California, Santa Barbara CA 93106, USA

We study the reach of the Large Hadron Collider with 1 fb^{-1} of data at $\sqrt{s} = 7$ TeV for several classes of supersymmetric models with compressed mass spectra, using jets and missing transverse energy cuts like those employed by ATLAS for Summer 2011 data. In the limit of extreme compression, the best limits come from signal regions that do not require more than 2 or 3 jets and that remove backgrounds by requiring more missing energy rather than higher effective mass.

I. INTRODUCTION

The Large Hadron Collider (LHC) is now testing the proposal that supersymmetry [1] (SUSY) is the solution to the hierarchy problem associated with the electroweak scale. At this writing, there have been no hints of supersymmetry, defying expectations based on the sensitivity of the Higgs potential to superpartner masses in many models, including the popular "mSUGRA" (minimal supergravity) scenario. It is possible that the failure of SUSY to appear is simply due to the up and down squarks being very heavy, as their production otherwise gives the strongest bounds. Another possibility is that the superpartners are not so heavy, but are difficult to detect because of a compressed mass spectrum, leading to much smaller visible energy than in mSUGRA benchmark cases. For our purposes here, compressed SUSY refers to the situation in which the mass ratio between the lightest supersymmetric particle (LSP) and the gluino is significantly smaller than the prediction $m_{\mathrm{LSP}}/m_{\tilde{g}} \sim 1/6$ of mSUGRA.

In a previous paper [2], we investigated the reach of 2010 data from ATLAS, consisting of 35 pb^{-1} of collisions at $\sqrt{s} = 7$ TeV, for several classes of compressed SUSY models. In the present work, we will update this analysis to correspond to the 1.04 fb^{-1} data set analyzed by ATLAS in

ref. [3]. Not only does this represent a huge increase in integrated luminosity, but also a revised set of signal regions compared to the 2010 data set analyses. The ATLAS analysis presents exclusion results for mSUGRA models, and for simplified models containing only squarks and a gluino but with the LSP mass held fixed at 0. In both cases the models tested are very far from the compressed case in which the mass difference between the gluino and the LSP is smaller. Our aims here are to see how the exclusions found for mSUGRA and simplified models translate into exclusions on compressed SUSY, for the various ATLAS signal regions, with particular attention to the exclusions that can be made in the most difficult case of very high compression. Other recent studies that include compressed SUSY and other non-mSUGRA searches at the LHC in a similar spirit can be found in [4]-[22].

The rest of this paper is organized as follows. Section II describes the signal regions and our procedures. Section III describes four classes of models, each of which depends on two parameters, the gluino mass $M_{\tilde{g}}$ and a compression parameter c, which are independently and continuously dialed to vary the overall superpartner mass scale and the ratio of gluino to LSP masses. Section IV gives results for the acceptances for these models with the various signal regions, and estimated exclusions based on the 1.04 fb^{-1} data set. Section V contains some concluding remarks.

II. PROCEDURES AND SIGNAL REQUIREMENTS

For this paper, we used the same tools as in our earlier work [2]. `MadGraph/MadEvent 4.4.62` [23] was used to generate hard scattering events using CTEQ6L1 [24] parton distribution functions, `Pythia 6.422` [25] for decays and showering and hadronization, and PGS 4 [26] for detector simulation. In SUSY models with compressed mass spectra, it is important to correctly generate jets beyond the hard scattering event, by matching correctly (without overcounting) between matrix-element and showering/hadronization software generation of additional jets. We did this by generating each lowest-order process together with the same process with one additional jet at the matrix-element level, followed by MLM matching with P_T-ordered showers with the shower-K_T scheme with $Q_{\mathrm{cut}} = 100$ GeV, as described in [27] and implemented in the MadGraph/MadEvent package. (It is much more time-consuming to include up to two extra jets at the matrix-element level. We found with some sample testing that it did not make a significant difference with our setup even for very compressed superpartner mass spectra.) For the detector simulation, we used the default ATLAS-like parameter card file provided with the PGS distribution, but with a jet cone size of $\Delta R = 0.4$. Cross-sections were normalized to the next-to-leading order output of `Prospino`

	A	B	C	D	E
Leading jet p_T [GeV]	> 130	> 130	> 130	> 130	> 130
Number of jets n	≥ 2	≥ 3	≥ 4	≥ 4	≥ 4
$p_T(j_n)$ [GeV]	> 40	> 40	> 40	> 40	> 80
m_{eff} [GeV]	> 1000	> 1000	> 500	> 1000	> 1100
$E_T^{\text{miss}}/m_{\text{eff}}$	> 0.3	> 0.25	> 0.25	> 0.25	> 0.2
ATLAS $\sigma \times$ Acc [fb]	< 22	< 25	< 429	< 27	< 17

TABLE I: Summary of cuts for the signals A, B, C, D, E simulated here, following the ATLAS 2011 data analyses for 1.04 fb^{-1} [3]. Also shown on the last line are the ATLAS 95% CL bounds on the non-Standard Model contribution to the cross-section times acceptance in the five signal regions. (In the case of signal region E only, the $m_{\text{eff}} > 1100$ GeV requirement involves a sum over all jets with $p_T > 40$ GeV, but the m_{eff} used in the $E_T^{\text{miss}}/m_{\text{eff}}$ cut is a sum over only the leading 4 jets.)

2.1 [28].

To define signals, we follow (a slightly simplified version of) the ATLAS cuts for multijets+E_T^{miss} from ref. [3]. The signal requirements are summarized in Table I. Events are required to have at least one jet with $p_T > 130$ GeV. The signal regions A, B, C, and D also require at least 2, 3, 4, and 4 jets with $p_T > 40$ GeV, respectively, while signal region E requires at least 4 jets with $p_T > 80$ GeV. These jets must have $|\eta| < 2.5$. The leading three jets are required to be isolated from the missing transverse momentum according to $\Delta\phi(\vec{p}_T^{\text{miss}}, j) > 0.4$. The effective mass m_{eff} is defined as the scalar sum of the E_T^{miss} and the p_T's of: the leading 2 jets for A; the leading 3 jets for B, the leading 4 jets for C, D; and all jets with $p_T > 40$ GeV for E. Then m_{eff} is required to exceed 1000, 1000, 500, 1000, and 1100 GeV respectively for signal regions A, B, C, D, E. In addition, a cut is imposed on the ratio $E_T^{\text{miss}}/m_{\text{eff}}$ of 0.3, 0.25, 0.25, 0.25, and 0.2 for A, B, C, D, E respectively. (For signal region E, only the 4 leading jet p_T's are summed over in the m_{eff} used in the $E_T^{\text{miss}}/m_{\text{eff}}$ cut, even though the m_{eff} cut uses an inclusive sum over jets.) Note that these cuts automatically imply a lower limit on E_T^{miss} of 300, 250, 125, 250 GeV for signals A, B, C, D, respectively. For signal region E, a cut $E_T^{\text{miss}} > 130$ GeV is imposed, although on an event-by-event basis this is usually superseded by the $E_T^{\text{miss}}/m_{\text{eff}}$ cut. There is a veto of events with leptons $\ell = (e, \mu)$ with $|\eta| < 2.4$ and (2.47) for muons (electrons), and $p_T^\ell > 20$ GeV that are farther than $\Delta R = \sqrt{(\Delta\eta)^2 + (\Delta\phi)^2} > 0.4$ from the nearest jet. Also shown on the last line of Table I are the ATLAS 95% CL limits on non-Standard-Model contributions to the signal regions after acceptance and efficiency, as reported in ref. [3]. These will be used below to estimate the reach for compressed SUSY models. ATLAS also has searches requiring higher jet multiplicities [29], leptons [30], and

b tagging [31], but these searches give significantly less reach for the compressed SUSY models we consider. Comparable searches by CMS have been reported in [32], [33], and [34]; we choose to use the ATLAS results only for reasons of convenience and familiarity.

Because our tools for generating SUSY signal events and simulating detector response are not the same as those used by ATLAS, the cross-section and acceptance results found below clearly cannot be interpreted in exact correspondence to the ATLAS ones. However, we have checked that the results of our analysis methods correlate well to those in ref. [3] for a sample of mSUGRA models used there. For mSUGRA models with $\tan\beta = 10$, $A_0 = 0$, $m_0 = 100$ GeV, and $m_{1/2} = 180$, 210, 240, 270, 300, 330, 360, 390, 420, 450, and 480 GeV, we found agreement with the ATLAS acceptance∗efficiency to be typically better than 15%, while for the same parameters but $m_0 = 660$ GeV, the agreement was usually at the 30% level or better. Keeping these inevitable differences in mind, at least an approximate estimate of the true detector response may still be gleaned from the results below, and the general trends should be robust.

III.   COMPRESSED SUSY MODELS

In this section, we define the compressed SUSY models for our study. Following our earlier work ref. [2], let us parameterize the electroweak gaugino masses at the TeV scale in terms of the gluino physical mass as

$$M_1 \; = \; \left(\frac{1 + 5c}{6}\right) M_{\tilde{g}}, \qquad M_2 \; = \; \left(\frac{1 + 2c}{3}\right) M_{\tilde{g}}. \tag{3.1}$$

Here c parameterizes the degree of compression. The value $c = 0$ gives an mSUGRA-like mass spectrum with gaugino masses approximately equal at $M_{\mathrm{GUT}} = 2.5 \times 10^{16}$ GeV, and $c = 1$ gives a completely compressed spectrum in which the gluino, wino, and bino masses are equal at the TeV scale. The gluino mass $M_{\tilde{g}}$ is treated as the independent variable input parameter that sets the superpartner mass scale. We also select $\tan\beta = 10$ and positive $\mu = M_{\tilde{g}} + 200$ GeV to compute the physical masses of charginos $\tilde{C}_i$ and neutralinos $\tilde{N}_i$. For our first class of models, we take the first- and second-family squark masses to be:

$$m_{\tilde{u}_R} = m_{\tilde{d}_R} = m_{\tilde{u}_L} = 0.96 M_{\tilde{g}}, \qquad m_{\tilde{d}_L}^2 = m_{\tilde{u}_L}^2 - \cos(2\beta) m_W^2, \tag{3.2}$$

and sleptons are taken degenerate with the squarks (so too heavy to appear in chargino and neutralino two-body decays). The top squark masses are taken to be $m_{\tilde{t}_1} = M_{\tilde{g}} - 160 + c(180 - 0.09 M_{\tilde{g}})$ and $m_{\tilde{t}_2} = M_{\tilde{g}} + 25$, in GeV. The lightest Higgs mass is fixed at $m_{h^0} = 115$ GeV, and
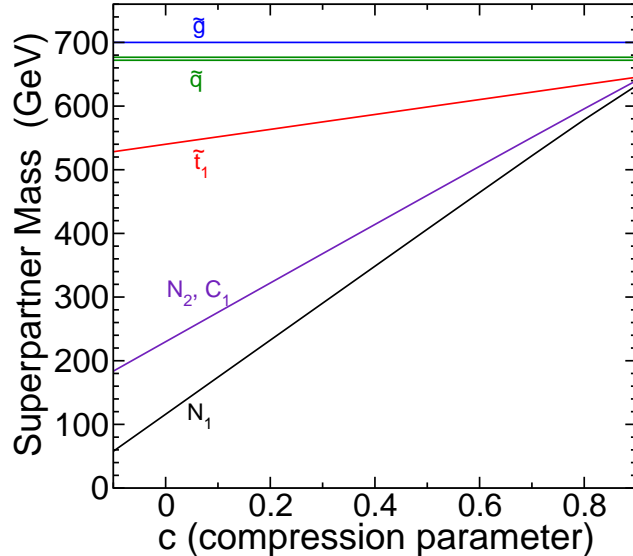
FIG. 1: The masses of the most relevant superpartners for the models of class I defined in section III, as a function of the compression parameter c, for fixed $M_{\tilde{g}} = 700$ GeV. The case $c = 0$ corresponds to an mSUGRA-like model.

the heavier Higgs masses with $m_{A^0} = 0.96 M_{\tilde{g}}$. These choices provide relatively smoothly varying branching ratios as the compression parameter c is varied, although transitions of $\tilde{N}_2$ and $\tilde{C}_1$ decays from on-shell to off-shell weak bosons are inevitable as the compression increases. In particular, the reason for the choice for the parameterization of the stop masses is to avoid suddenly turning on or off any 2-body decay modes as the parameter c is varied within each model line, by making sure that the the gluinos cannot decay to stops by kinematics for any of these models. The choices for $\tan\beta$ and μ are arbitrary, and not very much would change if they were modified (within some reasonable range). We refer to the two-parameter class of models spanned by varying $(M_{\tilde{g}}, c)$ as models I.

The masses of the most relevant superpartners are shown in Figure 1 for the case $M_{\tilde{g}} = 700$ GeV, illustrating the effect of the compression parameter c on the spectrum. In this class of models, gluino and squark production dominate at the LHC. The gluino decays mostly by the two-body mode $\tilde{g} \to \overline{q}\tilde{q}$ or $q\tilde{\overline{q}}$, and right-handed squarks decay mostly directly to the LSP, $\tilde{q}_R \to q\tilde{N}_1$, while left-handed squarks decay mostly to wino-like charginos and neutralinos, $\tilde{q}_L \to q'\tilde{C}_1$ and $q\tilde{N}_2$. The latter decay through on-shell or off-shell weak bosons: $\tilde{C}_1 \to W^{(*)}\tilde{N}_1$ and $\tilde{N}_2 \to Z^{(*)}\tilde{N}_1$, or $\tilde{N}_2 \to h\tilde{N}_1$ when it is kinematically allowed. The visible energy in each event from these decays clearly decreases as the compression factor c increases, because of the reduction in available kinematic phase space.

We define a second class of "heavy squark" models, II, which are the same as above but with

all squarks taken very heavy, $M_{\tilde{Q}} = M_{\tilde{g}} + 1000$ GeV. Thus when $c = 0$, the model classes I and II correspond approximately to mSUGRA with small and large m_0, respectively. In these heavy squark models, the most important production cross-section is from gluino pair production, with subsequent gluino decays $\tilde{g} \to \tilde{C}_1 q\bar{q}'$ and $\tilde{N}_2 q\bar{q}$ and $\tilde{N}_1 q\bar{q}$, with the first two typically dominating. The wino-like states then decay through on-shell or off-shell weak bosons, depending on the mass difference from the compression: $\tilde{C}_1 \to W^{(*)}\tilde{N}_1$ and $\tilde{N}_2 \to Z^{(*)}\tilde{N}_1$ or $h\tilde{N}_1$, with the last dominating if kinematically allowed.

One motivation for compressed SUSY is that taking M_3/M_2 much less than the mSUGRA prediction can significantly ameliorate [5, 35, 36] the supersymmetric little hierarchy problem. This provides motivation to consider compressed SUSY models in which winos are heavier than the gluino. Therefore, we define a third and fourth class of models, III ("heavy winos") and IV ("heavy winos and squarks"), to be the same as models I and II respectively, but with $M_2 = M_{\tilde{g}} + 100$ GeV in each case. In models III, all first- and second-family squarks decay directly to the LSP: $\tilde{q} \to q\tilde{N}_1$, while in models IV the squarks decouple from the discovery or best exclusion limit processes. The gluino has direct two-body decays to quarks and squarks as before.

The model classes I, II, and III were exactly those we used in ref. [2] in the context of limits obtainable with 35 pb^{-1} at LHC, while the model class IV corresponds approximately to the heavy squark limit of the simplified gluino/squark models in [3], but with neutralino LSP masses that are here non-zero and vary continuously with c. Thus the models that we discuss here provide a quite different slicing through the MSSM parameter space than those found in the experimental collaboration papers. We now proceed to use them to examine how the ATLAS exclusions on non-Standard Model cross-section times acceptance times efficiency impact the parameter space for SUSY with compressed mass spectra.

IV.   RESULTS OF SIMULATIONS

In compressed SUSY models, the visible energy in jets is reduced compared to mSUGRA models, leading to a significant reduction in acceptance for signal events. In Figure 2, we show the fractional acceptances after all cuts for the models in class I with $c = -0.1, 0, 0.1, \ldots, 0.9$ and $M_{\tilde{g}} = 300, 400, \ldots, 1300$ GeV. Results are shown for each of the signal regions A, B, D, and E. (We find that signal region C is not competitive for setting limits in any of the models we consider, see Figure 4 below, so it is not included in Figure 2.)

For fixed values of the mass difference $M_{\tilde{g}} - M_{\text{LSP}}$, the acceptance tends to approach a limit
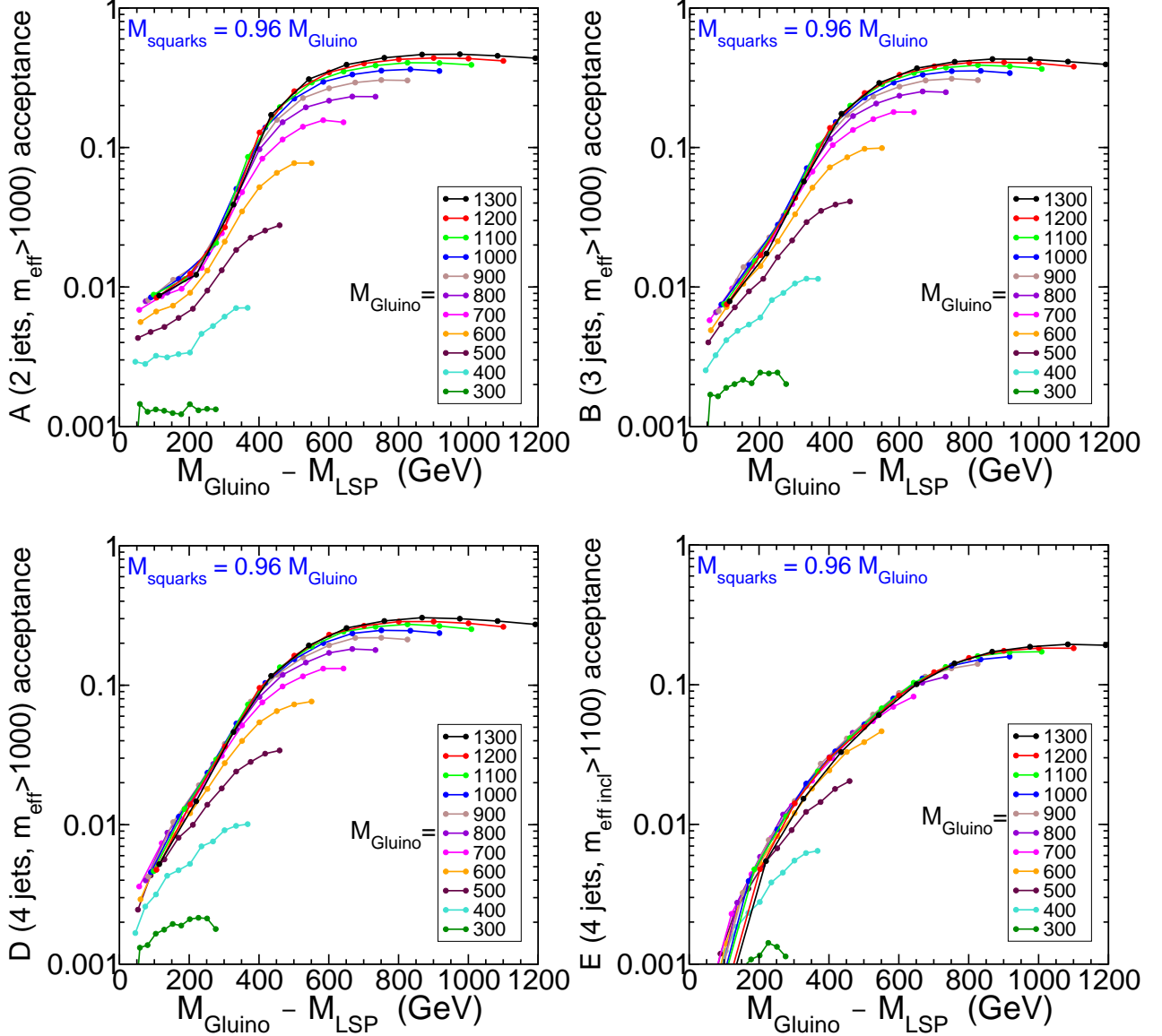
FIG. 2: Acceptances for the four signal regions A, B, D, E defined in Table I, for the class of models I defined in the text. The lines on each graph correspond to different values of the gluino mass. The dots on each line correspond to compression factors $c = -0.1, 0, 0.1, \ldots 0.9$ from right to left.

for sufficiently large $M_{\tilde{g}}$. Conversely, for sufficiently large $M_{\tilde{g}} - M_{\mathrm{LSP}}$, the acceptance tends to be relatively flat, but falls dramatically for $M_{\tilde{g}} - M_{\mathrm{LSP}} \lesssim 450$ GeV for signal regions A, B, and D, and for an even larger range of the mass difference for the high-mass signal region E. For severe compression $M_{\tilde{g}} - M_{\mathrm{LSP}} < 150$ GeV, the signal regions A and B can be seen to retain acceptance more than the signal regions D and E do, although in each case the acceptance declines to well below 1% for the most extreme compression, even when the gluino mass is very large.

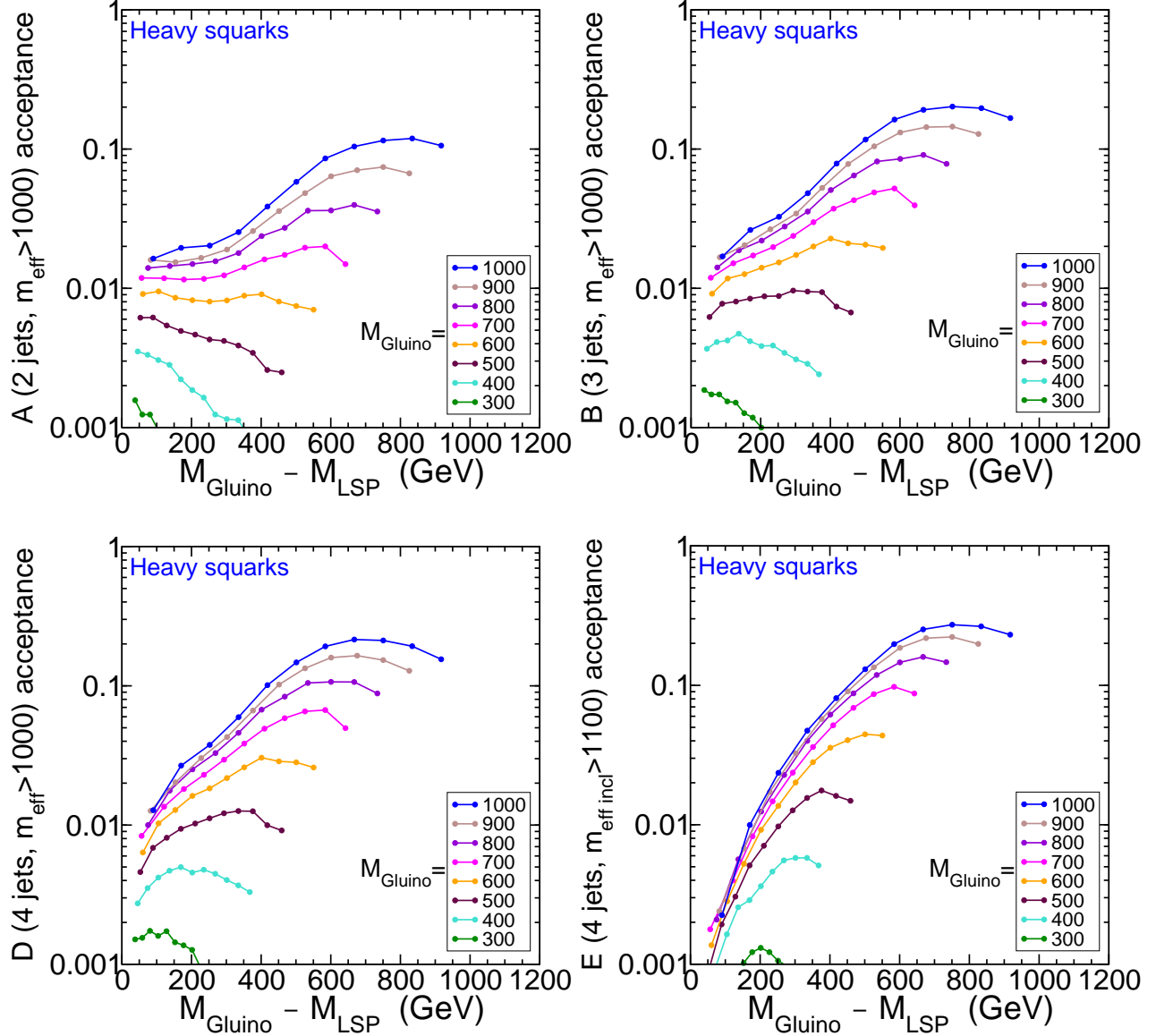The acceptances for the heavy squark models of class II are similarly shown in Figure 3 for

FIG. 3: As in Figure 2, but for the models II (heavy squarks) defined in the text.

gluino masses from 300 up to 1000 GeV. Here the acceptance tends to increase more steadily with increasing $M_{\tilde{g}}$. There is sometimes a notable decrease in acceptance for signal regions A and B as the mass difference $M_{\tilde{g}} - M_{\text{LSP}}$ increases, so that the largest acceptances are achieved with non-zero compression, that is, when $M_{\tilde{g}} - M_{\text{LSP}}$ is not maximum. This perhaps surprising effect, studied in [2], is due to the fact that as the compression increases, the m_{eff} distribution becomes soft faster than the E_T^{miss} distribution does, so that more events pass the $E_T^{\text{miss}}/m_{\text{eff}}$ cuts.

The acceptances for models in classes III (heavy winos) and IV (heavy squarks and winos) are qualitatively similar, and so are not shown.

In Figure 4, we show contours of cross-section times acceptance for all five signal regions, for

each of the model classes I, II, III, IV in separate panels. The contours for each signal region are for the corresponding ATLAS limits on non-Standard Model processes listed in Table I (taken from [3]), so that the regions to the left of each contour may be regarded as the approximate exclusion regions for that signal definition. In the panels for model classes I and II, the (orange) dotted line indicates the case $c = 0$ in which the ratio of gaugino masses at the TeV scale is approximately the same as mSUGRA. For the light squark class of models I, the best signal regions for exclusion are A (when $M_{\tilde{g}} - M_{\mathrm{LSP}} > 400$ GeV) and B (for most of the range of smaller mass differences, except for the most extremely compressed case).

Signal regions A and B likewise give the best exclusions for models in class III (heavy winos but light squarks). Because the gluino and squark decays in this class of models do not pass through the intermediate cascade step of winos, the visible energy per jet tends to be larger, leading to stronger exclusions as shown. In both of the model classes I and III with squarks slightly lighter than the gluino, we find that even in the case of extreme compression one can still set a limit of better than $M_{\tilde{g}} > 600$ GeV.

In models with heavy squarks, the limits are much worse, since the main SUSY production is only gluino pairs. For models of class II with heavy squarks and light winos, the best limit is set using the high-mass signal region E when $M_{\tilde{g}} - M_{\mathrm{LSP}} > 200$ GeV. For smaller mass differences, the 3-jet signal region B sets better limits, because the m_{eff} distribution for the signal events becomes too soft. Still, it should be possible to set a limit of about $M_{\tilde{g}} > 450$ GeV using signal regions A and B, even in the case of extreme compression with $c = 0.9$. Qualitatively similar statements apply to models in class IV with both squarks and winos decoupled. Note than in all cases, signal region C is comparatively ineffective in setting limits, because the backgrounds are too large.
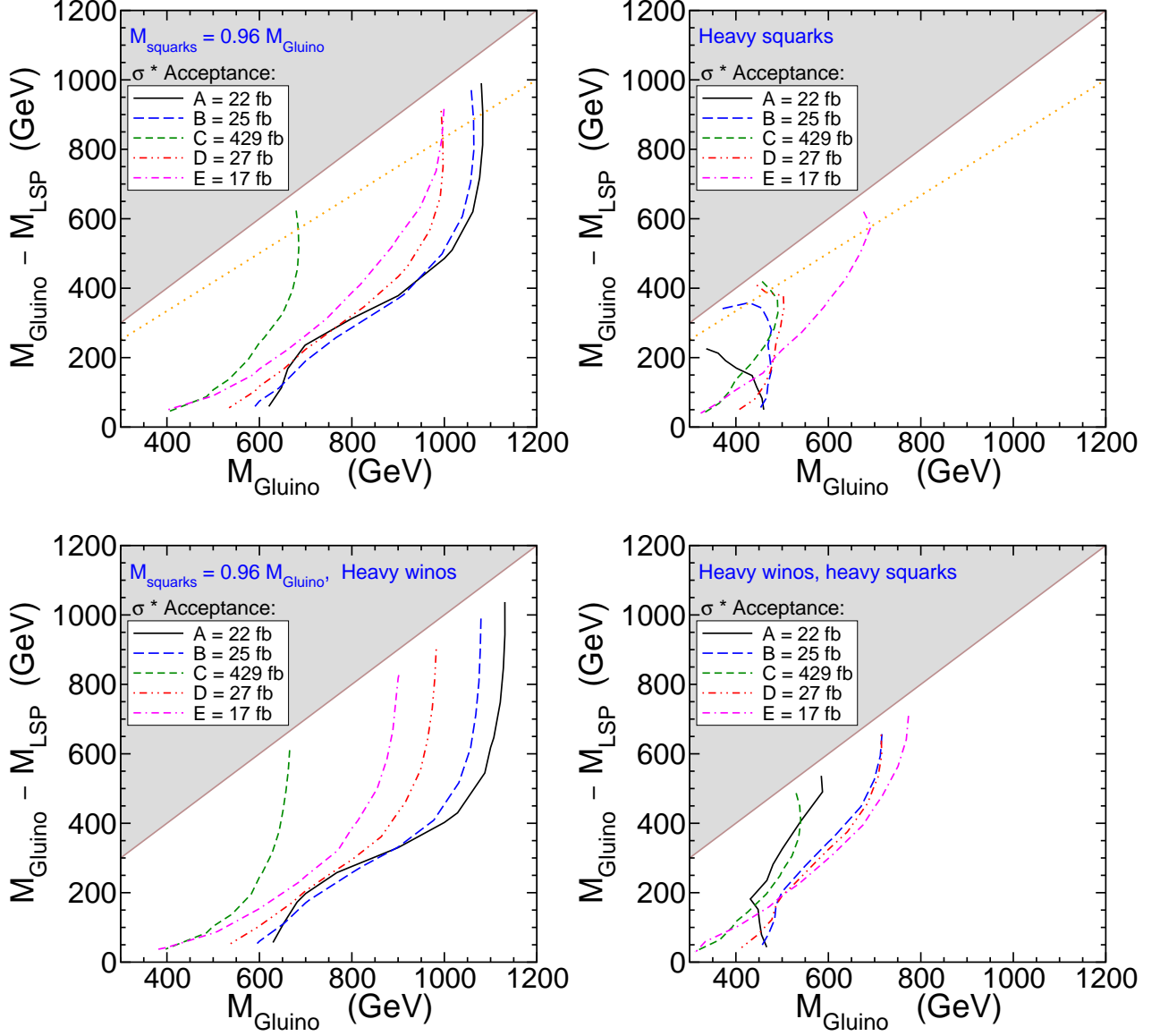
FIG. 4: Contours of constant cross-section times acceptance for the five signal regions defined in Table I, in the $M_{\tilde{g}} - M_{\tilde{N}_1}$ vs. $M_{\tilde{g}}$ plane obtained by varying the gaugino mass compression parameter c between -0.1 and 0.9. The four panels correspond to the models I (light squarks), II (heavy squarks), III (heavy winos), and IV (heavy winos and heavy squarks). The dotted lines in the first two cases corresponds to the mSUGRA-like case $c = 0$. Increased compression is lower in each plane.
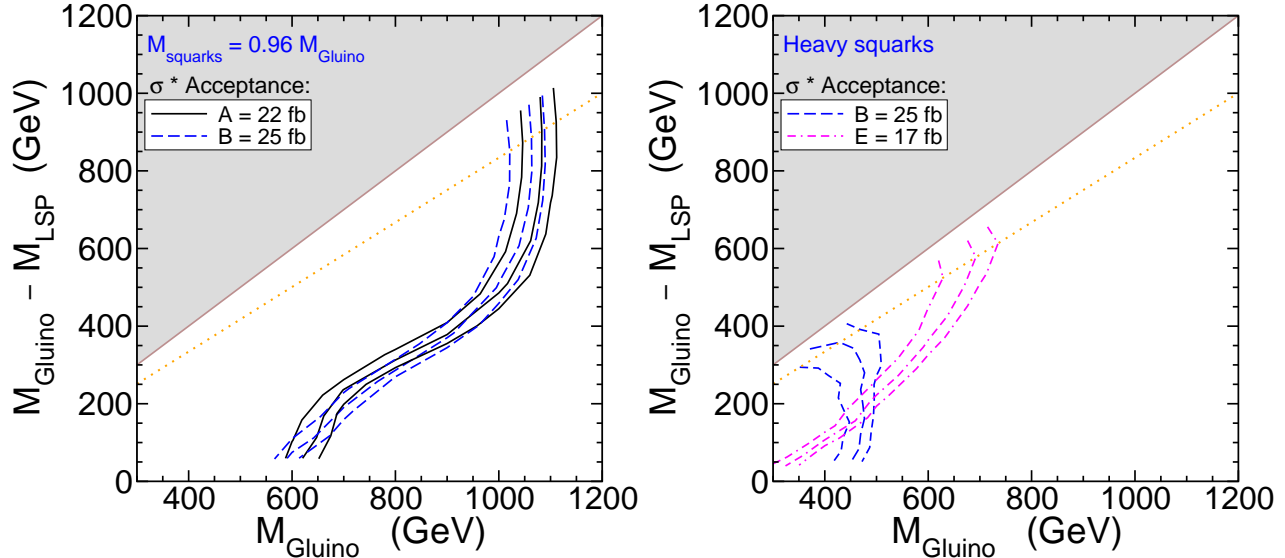
FIG. 5: The impact of systematic uncertainties in the signal rates on contours of constant cross-section times acceptance for selected signal regions. The middle line in each case is the same result as in Figure 4. The corresponding left and right contours show the impact of decreasing and increasing the total signal production rate by 25%. The two panels correspond to the models I (light squarks, left) and II (heavy squarks, right).

The preceding results were all obtained using the Prospino NLO default renormalization and factorization scale choices and without taking into account the possible systematic uncertainties in the signal production cross sections. In general, uncertainties in QCD production cross-sections are notoriously difficult to estimate. It is well-known that variation of renormalization and factorization scales and PDFs do not give reliable estimates of the production cross-section uncertainties. To illustrate the potential impacts of these uncertainties, we show in Figure 5 how the results vary when changing the assumed total signal cross-section by $\pm 25\%$ for the models of class I and II. Only the two signal regions that give the strongest limits over the most significant ranges of $M_{\tilde{g}} - M_{\mathrm{LSP}}$ are shown in each case. This variation results in a change in the gluino mass limit in these models that can exceed ± 50 GeV, depending on the model parameters.

V.   OUTLOOK

In this paper, we have studied the reach of 1 fb^{-1} of LHC data at $\sqrt{s} = 7$ TeV for compressed SUSY models, extending our earlier results for 35 pb^{-1} in [2]. We found that even in the most compressed case studied, in which the gluino is only about 9% heavier than the LSP, the limit on the gluino mass should be about $M_{\tilde{g}} > 600$ GeV for squarks that are slightly lighter than the gluino, and

about $M_{\tilde{g}} > 450$ GeV when squarks are very heavy. The best limits (and discovery potential) come from signal regions which require 2 or 3 jets. In designing future searches for compressed SUSY, it is probable that the best reach will be obtained by increasing the cut on E_T^{miss} as necessary to reduce the backgrounds, rather than by very hard cuts on m_{eff} (or H_T). This is because as the compression increases, both the E_T^{miss} and m_{eff} distributions get softer, but the latter more drastically. (A more precise quantitative statement about this is beyond the scope of this paper, since it would require detailed background estimates including crucially detector response-specific information.) Future searches should take into account that signal regions optimized for mSUGRA and for simplified models with massless or light LSPs will therefore not do very well for compressed SUSY models, and this effect will become more significant as higher mass scales are probed.

[1] For reviews of supersymmetry at the TeV scale, see S.P. Martin, "A supersymmetry primer," [hep-ph/9709356] (version 5, December 2008). M. Drees, R. Godbole and P. Roy, "Theory and phenomenology of sparticles: An account of four-dimensional N=1 supersymmetry in high energy physics," *World Scientific (2004).* H. Baer and X. Tata, "Weak scale supersymmetry: From superfields to scattering events," *Cambridge University Press (2006).*

[2] T.J. LeCompte, S.P. Martin, Phys. Rev. **D84**, 015004 (2011). [arXiv:1105.4304 [hep-ph]].

[3] G. Aad *et al.* [ATLAS Collaboration], "Search for squarks and gluinos using final states with jets and missing transverse momentum with the ATLAS detector in sqrt(s) = 7 TeV proton-proton collisions," arXiv:1109.6572 [hep-ex]. See also `http://hepdata.cedar.ac.uk/view/p8082`

[4] H. Baer, A. Box, E.K. Park and X. Tata, JHEP **0708**, 060 (2007) 0707.0618 [hep-ph].

[5] S.P. Martin, Phys. Rev. **D78**, 055019 (2008). 0807.2820 [hep-ph].

[6] J. Alwall, M.-P. Le, M. Lisanti, J.G. Wacker, Phys. Rev. **D79**, 015005 (2009). [arXiv:0809.3264 [hep-ph]].

[7] D.S.M. Alves, E. Izaguirre and J.G. Wacker, "It's On: Early Interpretations of ATLAS Results in Jets and Missing Energy Searches," Phys. Lett. **B702**, 64-68 (2011), 1008.0407 [hep-ph];

[8] J.A. Conley, J.S. Gainer, J.L. Hewett, M.P. Le and T.G. Rizzo, Eur. Phys. J. **C71**, 1697 (2011), 1009.2539 [hep-ph]; "Supersymmetry without prejudice at the 7 TeV LHC," 1103.1697 [hep-ph].

[9] S. Scopel, S. Choi, N. Fornengo and A. Bottino, Phys. Rev. **D83**, 095016 (2011) 1102.4033 [hep-ph].

[10] O. Buchmueller *et al.*, Eur. Phys. J. C **71**, 1634 (2011) 1102.4585 [hep-ph]. See also P. Bechtle *et al.*, Phys. Rev. **D84**, 011701 (2011) arXiv:1102.4693 [hep-ph] for a similar study within mSUGRA.

[11] D.S.M. Alves, E. Izaguirre, J.G. Wacker, JHEP **1110**, 012 (2011). [arXiv:1102.5338 [hep-ph]].

[12] S. Akula, D. Feldman, Z. Liu, P. Nath and G. Peim, Mod. Phys. Lett. **A26**, 1521-1535 (2011). [arXiv:1103.5061 [hep-ph]].

[13] D. Alves, *et al.*, "Simplified Models for LHC New Physics Searches," [arXiv:1105.2838 [hep-ph]].

[14] J. Fan, M. Reece and J. T. Ruderman, JHEP **1111**, 012 (2011) [arXiv:1105.5135 [hep-ph]].

[15] O. Buchmueller *et al.*, "Supersymmetry in Light of 1/fb of LHC Data," [arXiv:1110.3568 [hep-ph]], Eur. Phys. J. **C71**, 1722 (2011). [arXiv:1106.2529 [hep-ph]].

[16] M. A. Ajaib, T. Li, Q. Shafi, Phys. Lett. **B705**, 87-92 (2011). [arXiv:1107.2573 [hep-ph]].

[17] S. Sekmen *et al.*, "Interpreting LHC SUSY searches in the phenomenological MSSM," [arXiv:1109.5119 [hep-ph]].

[18] B. C. Allanach, T. J. Khoo, K. Sakurai, "Interpreting a 1 fb^-1 ATLAS Search in the Minimal Anomaly Mediated Supersymmetry Breaking Model," [arXiv:1110.1119 [hep-ph]].

[19] A. Arbey, M. Battaglia, F. Mahmoudi, "Implications of LHC Searches on SUSY Particle Spectra: The pMSSM Phase Space with Neutralino Dark Matter," [arXiv:1110.3726 [hep-ph]].

[20] R. Essig, E. Izaguirre, J. Kaplan, J.G. Wacker, "Heavy Flavor Simplified Models at the LHC," [arXiv:1110.6443 [hep-ph]].

[21] Y. Kats, P. Meade, M. Reece, D. Shih, "The Status of GMSB After 1/fb at the LHC," [arXiv:1110.6444 [hep-ph]].

[22] M. Papucci, J.T. Ruderman, A. Weiler, "Natural SUSY Endures," [arXiv:1110.6926 [hep-ph]].

[23] J. Alwall *et al.*, JHEP **0709**, 028 (2007) F. Maltoni and T. Stelzer, "MadEvent: Automatic event generation with MadGraph," JHEP **0302**, 027 (2003) [hep-ph/0208156], T. Stelzer and W. F. Long, Comput. Phys. Commun. **81**, 357 (1994) [hep-ph/9401258].

[24] J. Pumplin *et al.*, JHEP **0207**, 012 (2002) [hep-ph/0201195].

[25] T. Sjostrand, S. Mrenna and P. Skands, JHEP **0605**, 026 (2006) [hep-ph/0603175].

[26] John Conway et al., "PGS4: Pretty Good Simulation of high energy collisions", `http://www.physics.ucdavis.edu/~conway/research/software/pgs/pgs4-general.htm`.

[27] `http://cp3wks05.fynu.ucl.ac.be/twiki/bin/view/Main/IntroMatching`. See also J. Alwall, S. de Visscher and F. Maltoni, JHEP **0902**, 017 (2009) 0810.5350 [hep-ph]. J. Alwall *et al.*, Eur. Phys. J. C **53**, 473 (2008) 0706.2569 [hep-ph].

[28] Prospino 2.1, available at `http://www.ph.ed.ac.uk/~tplehn/prospino/`, uses results found in: W. Beenakker, R. Hopker, M. Spira and P.M. Zerwas, Nucl. Phys. B **492**, 51 (1997) [hep-ph/9610490], W. Beenakker et al, Nucl. Phys. B **515**, 3 (1998) [hep-ph/9710451], W. Beenakker et al, Phys. Rev. Lett. **83**, 3780 (1999) [Erratum-ibid. **100**, 029901 (2008)] [hep-ph/9906298], M. Spira, [hep-ph/0211145], T. Plehn, Czech. J. Phys. **55**, B213 (2005) [hep-ph/0410063].

[29] G. Aad *et al.* [ATLAS Collaboration], "Search for new phenomena in final states with large jet multiplic-

ities and missing transverse momentum using sqrt(s)=7 TeV pp collisions with the ATLAS detector," arXiv:1110.2299 [hep-ex].

[30] G. Aad *et al.* [ATLAS Collaboration], "Search for supersymmetry in final states with jets, missing transverse momentum and one isolated lepton in sqrts = 7 TeV pp collisions using 1 fb^{-1} of ATLAS data," arXiv:1109.6606 [hep-ex] and "Searches for supersymmetry with the ATLAS detector using final states with two leptons and missing transverse momentum in sqrts = 7 TeV proton-proton collisions," arXiv:1110.6189 [hep-ex].

[31] The ATLAS Collaboration, "Search for supersymmetry in pp collisions at sqrt(s) = 7 TeV in final states with missing transverse momentum, b-jets and one lepton with the ATLAS detector" ATLAS-CONF-2011-130, "Search for supersymmetry in pp collisions at sqrt(s) = 7 TeV in final states with missing transverse momentum, b-jets and no leptons with the ATLAS detector", ATLAS-CONF-2011-098.

[32] S. Chatrchyan *et al.* [CMS Collaboration], "Search for Supersymmetry at the LHC in Events with Jets and Missing Transverse Energy," arXiv:1109.2352 [hep-ex]. "Search for supersymmetry in all-hadronic events with missing energy", the CMS Collaboration, CMS-PAS-SUS-11-004. "Search for supersymmetry in all-hadronic events with MT2", the CMS Collaboration, CMS-PAS-SUS-11-005.

[33] The CMS Collaboration, "Search for new physics with same-sign isolated dilepton events with jets and missing energy", CMS-PAS-SUS-11-010; "Search for new physics in events with opposite-sign dileptons and missing transverse energy", CMS-PAS-SUS-11-011; "Searches for Supersymmetry using Multilepton Signatures in pp Collisions at 7 TeV", CMS-PAS-SUS-11-013; "Search for supersymmetry in events with a lepton and missing energy" CMS-PAS-SUS-11-015.

[34] The CMS Collaboration, "Search for New Physics in Events with b-quark Jets and Missing Transverse Energy in Proton-Proton Collisions at 7 TeV", CMS-PAS-SUS-11-006.

[35] G.L. Kane and S.F. King, Phys. Lett. B **451**, 113 (1999) [hep-ph/9810374], M. Bastero-Gil, G.L. Kane and S.F. King, Phys. Lett. B **474**, 103 (2000) [hep-ph/9910506].

[36] S.P. Martin, Phys. Rev. D **75**, 115005 (2007) [hep-ph/0703097], Phys. Rev. D **76**, 095005 (2007) [hep-ph/0707.2812].